Similarity-based versus Template Matching-based Methodologies for Image Alignment of Polyhedral-like Objects under Noisy Conditions

LÚCIO DE SOUZA COELHO

MÁRIO FERNANDO MONTENEGRO CAMPOS

Departamento de Ciência da Computação - ICEX - UFMG
Av. Antônio Carlos, 6627, Pampulha, CEP 31270-010, Belo Horizonte - MG, Brazil
{omni,mario}@dcc.ufmg.br

Abstract. The image alignment problem has as input a set of different images from a single object or several identical objects. One instance of the object in each image is misaligned relatively to the other in a given image, that is, the objects lie in different positions and orientations. Thus, the problem consists in finding the homogeneous planar transforms for each of those instances. The process is not simple in the case of noisy images. Nevertheless, it is possible to tackle some cases of the image alignment problem using template matching. This work describes two methodologies that were developed to align noisy images of protein quaternary structures obtained by Transmission Electron Microscopy (TEM). These structures can be geometrically described by regular prisms and polyhedra. One of the methods uses the traditional approach for this problem -- exploring image similarities. The second one explores the geometric simplicity of the objects being imaged by using template matching in order to solve the problem. The results show that there are cases where the template matching method achieves higher precision and computational efficiency to align that kind of image when compared to traditional ones.

Keywords: template matching, geometric modeling, biological applications.

1 Introduction

Several Computer Vision [Ballard and Brown (1982)] and Digital Image Processing [Castleman (1979)] applications, such as 3D reconstruction of proteins from electron micrographs [Radermacher (1992)], deal with the image alignment problem in one or more steps of their implementations .

The image alignment problem has as input a set of images of the same object or of identical objects. In each image, there is a instance of the object in a different position and orientation. The problem is to estimate the planar position and orientation of the object in each image. Once they are known, homogeneous planar transforms are calculated for each image in order to give as result images where the object appears in the same position and orientation.

A generic solution for this problem can be achieved by exploring image similarities. However, this approach is not trivial when imaging is done under noisy conditions; in this situation, the images of the same object are unlike enough to difficult similarity matches. Also, the usual similarity method chooses a reference image to which all others are aligned to [Harauz and Boekema (1992)]. So one has to carefully choose the reference image since a wrong choice can incorrectly bias the alignment of the whole set.

Nevertheless, it is possible to accomplish better solutions to the image alignment problem when some previous knowledge about the imaged objects is available. That knowledge can be a set of geometric models, or templates, of the objects. In this case, the image alignment problem can be solved by using well known techniques such as *template matching* [Rosenfeld and Kak (1982)]. After matching a template to the images to be aligned, the solution to the problem is straightforwardly obtained by recovering the transforms that describe the template position and orientation in each image.

An example of a class of objects that can be described by templates is that composed by quaternary protein structures . Such biomolecular complexes can be geometrically described in terms of regular polyhedra and prisms [Gilbert (1976)], as depicted on Figure 1. In particular, the icosahedral template also fits to bigger protein assemblies, the icosahedral virus capsids [Stannard (1995)].

The shape of such objects is of great biological importance and can be determined by 3D reconstruction from TEM images. However, even large molecules as proteins are close to the resolution limit of TEM, and the imaged structures are very noisy, as shown in Figure 2.

The sixfold prismatic shape of the proteins presented there is clearly perceived. However, it also can be noticed that not only the noise-to-signal ratio of the image is high, but also the background is somewhat heterogeneous. These combined factors contributes to a low similarity between images of the protein in the same characteristic view. Fortunately, the signal-to-noise ratio of TEM images of such objects can be reduced by the image averaging technique. This technique consists in creating a high-resolution image from a great number of images of identical molecular assemblies in the micrograph by averaging the intensities of their corresponding pixels. Clearly this method requires that all images are aligned. Traditionally, this alignment is performed based on image similarity, such as correlation function-based procedures [Van Heel et al. (1995)].
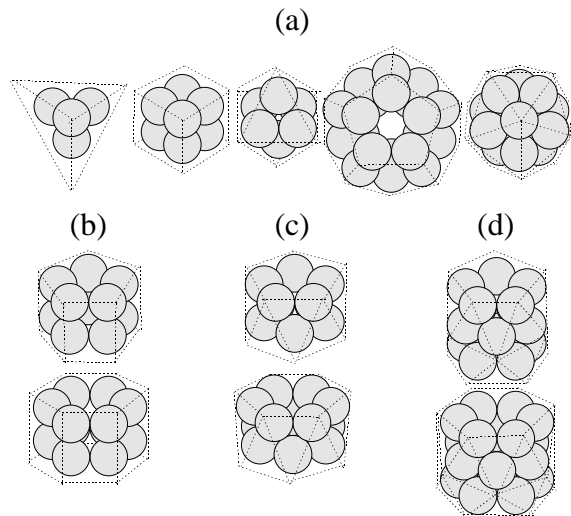
Figure 1: the basic geometric models for quaternary protein structures. They can assume configurations such as (a) regular polyhedra; (b) regular prisms; (c) twisted regular prisms and (d) double-twisted regular prisms.

As pointed out before, TEM images of such objects however are suitable for alignment by template matching. In particular, the sample preparation technique known as *negative staining* [Steven and Navia (1980)] guarantees that every structure in a micrograph lies on a plane, which already imposes constraints in their orientations. The typical views then can be matched by simple planar templates allowing for an easy implementation of reasonable computational cost.

This work proposes the application of template matching in order to achieve better results to the alignment of TEM images. It will be restricted to negatively stained

quaternary protein structures and some species of icosahedral virus. The efficiency of the method in terms of computational cost and quality of the final result is measured and compared with those achieved by a similarity-based image alignment methodology. The following sections give a more precise definition of the image alignment problem and the geometric constraints of the type of image described here. It also describes both template-matching methodology proposed here and the similarity method which is used for comparison purposes. Results of both methodologies are shown and discussed.
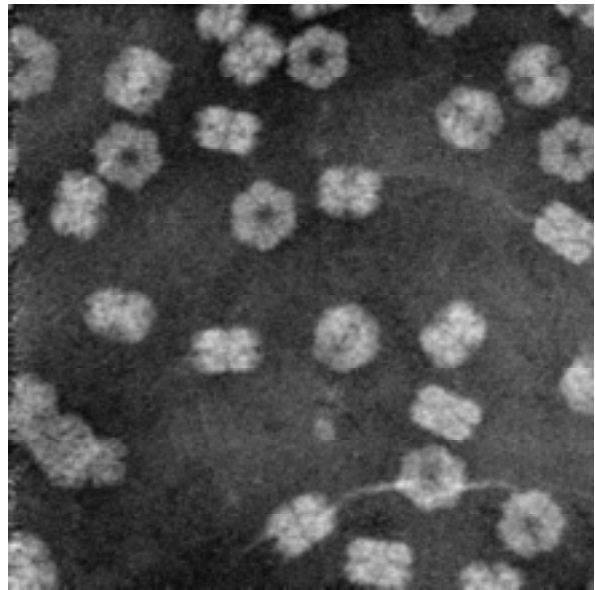
Figure 2: transmission electron micrograph of a negatively stained sample of earthworm hemoglobin molecules. Downloaded from the web site of the Biology Department of the Brookhaven National Laboratory (http://bnlstb.bio.bnl.gov/).

2 Definition of the Problem

In this section, the image alignment problem is defined. The geometrical constraints of protein quaternary structures and their orientations on a negatively stained sample are also formally described.

2.1 The Image Alignment Problem

Let O be an object with an attached orientation vector $\vec{v}$. O lies on an imaging plane parallel to $\vec{v}$. Let A be an ordered set of n images. Each image $a_i \in A$ has been obtained by imaging O with the same device D. For each a_i, O is rotated and translated along the imaging plane by a planar transform $\mathbf{T}_i$, yielding a set of corre-

sponding orientation vectors $\vec{v}_i = \mathbf{T}_i \vec{v}$. Thus, the image alignment problem is to find another ordered set S of n transforms where

$$\forall \mathbf{S}_i, \mathbf{S}_j \in S, i \neq j, \mathbf{S}_i \vec{v}_i = \mathbf{S}_j \vec{v}_j.$$

That is, the application of S to A aligns the images in A, where O will have the same position and orientation in all images. The set of these aligned images is the solution for the problem. Figure 3 depicts the configuration of one instance of this problem and its solution.

Although the mathematical definition of the problem deals with an orientation vector intrinsic to the object, that vector is not previously known in real problems.

2.2 The Orientation of Polyhedra on Planes

A homogeneous density for the quaternary protein structures is assumed. (Actually, that density is not homogeneous. However, density variations are symmetrically distributed along the volume of protein quaternary structures. Hence, the assumption of uniform density does not invalidate the following discussion.) The quaternary protein structures are geometrically modeled here as simple polyhedra of the following classes.

Regular Solids: regular tetrahedra, cubes, octahedra, dodecahedra and icosahedra.

Regular Prisms: prisms with $n + 2$ faces where n faces are rectangles and two faces are regular polygons with n sides.

Twisted Regular Prisms: polyhedra with $2n + 2$ where $2n$ faces are isosceles triangles and 2 faces are regular polygons.

Double-Twisted Regular Prisms: polyhedra with $4n + 2$ where $4n$ faces are isosceles triangles and 2 faces are regular polygons.

The orientation of the defined polyhedra on a plane, considering the effect of a gravitational field perpendicular to that plane, is now discussed. (The same discussion is valid considering any other attractive force between the molecule and the imaging plane, like intermolecular interactions.) Clearly, the set of stable orientations for the polyhedra includes only orientations where a face of the polyhedron coincides with the imaging plane. The stability of such orientations also requires that the projection of the geometric center of the polyhedron on the imaging plane lies inside the face that coincides with the plane.

Thus, since those constraints are posed to polyhedral orientation, it is easily seen that the set of projections of the polyhedra on the plane is also limited. For instance, a regular prism has only as projections regular polygons and rectangles. For regular solids the projections are even simpler, being only regular polygons.
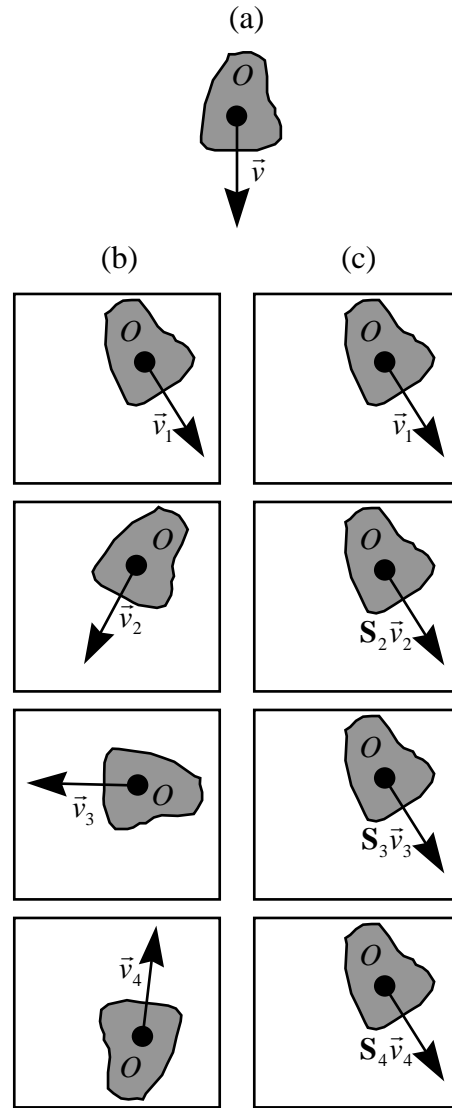
Figure 3: an instance of the image alignment problem and a solution. In (a), the object O is shown with an attached vector $\vec{v}$. In (b), several images of O in different planar orientations are displayed as well as the corresponding $\vec{v}_i$ vectors. Finally, a solution is shown in (c); notice that the first image remains unchanged, because it was used as a reference.

3 The Methodologies

The aforementioned approaches to the image alignment problem case discussed in this paper are formally de-

scribed in this section. The similarity-based algorithm, as well as the template matching-based one, are presented and their complexities are analyzed.

However, a simple framework is firstly presented for both methodologies. This framework handles the discrete nature of images and their transforms. Gray-level images [Pavlids (1982)] (represented as matrices of intensities ranging in the set $\{0,1,2,...,255\}$) will be used here. It is assumed that all images in the ordered input set of images A are *isomorphic* to each other, that is, have the same height and width, given respectively by functions $h(A)$ and $w(A)$. Planar image transforms are implemented in an "inverse way", that is, to each pixel of the output image it is assigned the intensity of the corresponding pixel in the input image; this approach is used to provide antialiasing [Rogers (1985)]. Also, rotations and translations are performed separately, such that rotations are defined around the viewing axis by an amount α with respect to the coordinate (x,y), denoted by the operator $R_z(\alpha,(x,y))$ (adapted from [Craig (1989)]).

3.1 The Similarity-Based Method

The similarity-based image alignment method described here is basically an exhaustive search algorithm operating in a discrete space of orientations. It determines the best reference image by trying each $a_i \in A$ as a reference image.

For each a_i, the center of mass of the other images are superimposed to the center of mass of a_i by means of translations. The center of mass $m(a)$ of an image $a \in A$ is given by

$$m(a) = \left(\frac{\sum_{x=1}^{w(A)}\sum_{y=1}^{h(A)} x a[x,y]}{\sum_{x=1}^{w(A)}\sum_{y=1}^{h(A)} a[x,y]}, \frac{\sum_{x=1}^{w(A)}\sum_{y=1}^{h(A)} y a[x,y]}{\sum_{x=1}^{w(A)}\sum_{y=1}^{h(A)} a[x,y]} \right)$$

The application of a translation on an image b in order to superimpose its center of mass to that of an image a will be denoted as $m(a,b)$. Once the mass centers are superimposed, each $a_{j\neq i} \in A$ is rotated in all possible ways modulo the discrete representation. The best orientation for the current image is chosen by the criterion of minimum Euclidean distance [Machado (1994)] to the reference image. That distance between two images a and b is denoted as $d(a,b)$. The best reference image yields the

minimum sum of minimum Euclidean distances to the other images. Then, the best transforms for the best reference image are considered the solution for the problem. A high-level description of the algorithm is given below:

1. $M \leftarrow 255n\sqrt{w(A)h(A)}$.

2. $C \leftarrow \{c_1, c_2, ..., c_n\}$.

3. $B \leftarrow \{b_1, b_2, ..., b_n\}$.

4. $d\alpha \leftarrow \arctan(2 / \min(h(A), w(A)))$.

5. For i from 1 to n repeat steps 6 to 12.

6. $b_i \leftarrow a_i$.

7. For all $a_{j\neq i}$ repeat steps 8 to 12.

8. $m \leftarrow M / n$.

9. While $\alpha < 2\pi$ repeat steps 10 to 11.

10. if $\quad d\Big(a_i, R_z\Big(\alpha, \overline{m}\big(\overline{m}(a_i, a_j)\big)\Big)\overline{m}(a_i, a_j)\Big) < m \qquad$ then

$\quad m \leftarrow d\Big(a_i, R_z\Big(\alpha, \overline{m}\big(\overline{m}(a_i, a_j)\big)\Big)\overline{m}(a_i, a_j)\Big) \qquad$ and

$\quad b_j \leftarrow R_z\Big(\alpha, \overline{m}\big(\overline{m}(a_i, a_j)\big)\Big)\overline{m}(a_i, a_j)$.

11. $\alpha \leftarrow \alpha + \partial\alpha$.

12. if $\quad \sum_{j\neq i} d(a_i, b_j) < M \quad$ then $\quad M \leftarrow \sum_{j\neq i} d(a_i, b_j) \quad$ and

$\quad C \leftarrow B$.

At the end of the execution of the algorithm, the best solution found for the image alignment problem is stored in C.

An operation suitable for measuring the complexity of the algorithm is the number of distance measurements. In order to estimate that number, the number of measurements in a image scanning is first determined. An image scanning is the measurement of the distances between images considering all rotations relevant to the discrete representation used. Putting in another way, a image scanning corresponds to steps 9 and 10 of the algorithm. Thus, the number of measurements during an image scanning is about

$$t = \frac{2\pi}{\arctan(1 / \max(h(A), w(A)))} .$$

The total number of image scannings performed by the algorithm is $n(n-1)$. Hence, the complexity of the algorithm is $O(n^2 t)$ on the number of distance measurements.

3.2 The Template-Based Method

The template-based method operates individually in each image instead of experiencing all possible correlations between images as the similarity-based method does. For each image, the method performs basically two steps. The first one is the extraction of edges in the image to be aligned. The second step is the scanning of the image with the template with all possible sizes, orientations and positions under the discrete framework used. The transform (size, orientation and position) that provides the best match between the template and the edges of the original image is chosen. Those concepts are formally defined next.

A non-linear edge detector is used for edge extraction. Using that detector, $e(a)$, the edge extraction image of a given image a, has its pixel intensities defined by

$$e(a)[x,y] = \max_{h,v \in \{-1,0,1\}} |a[x,y] - a[x+h, y+v]|,$$

for those pixels x,y that are not part of the image border; otherwise, $e(a)[x,y] = 0$.

The case of regular polygonal templates is discussed in detail. In terms of representation, such templates are *binary images* [Barrera and Banon (1994)]. The template of a regular polygon of diameter Δ and with f sides is a binary image $p(\Delta, f)$ with $\Delta \times \Delta$ pixels with the polygon drawn by one-pixel lines centered in the image.

The *matching* $m(a,b)$ between a binary image b and a gray-level image a is measured as the sum of intensities of the pixels of a that correspond to true (white) pixels in b. b is shifted relatively to a by a vector (h,v). The matching is then defined as

$$m(a,b,(h,v)) = \sum_{b[x,y]=1} a[x+h, y+v].$$

This matching is used here to evaluate how good a template (rotated and/or translated) adjusts to the edges of an image.

Finally, the *shifting* of an image a by h pixels along the horizontal direction and v pixels along the vertical direction is denoted as $[h,v]a$.

With the above definitions, the high-level algorithm for the template-based method (considering a regular polygonal template) is presented below:

1. $C \leftarrow \{c_1, c_2, ..., c_n\}$.
2. For i from 1 to n repeat steps 3 to 12.
3. $M \leftarrow 0$.
4. For Δ from $\min(w(A), h(A))$ down to 3 repeat steps 5 to 12.
5. $\alpha \leftarrow 0$.
6. $d\alpha \leftarrow \arctan(2/\Delta)$.
7. While $\alpha < 2\pi/f$ repeat steps 8 to 12.
8. $b \leftarrow R_z(\alpha, (\Delta/2, \Delta/2)) p(\Delta, f)$.
9. For x from 1 to $w(A) - \Delta$ repeat steps 10 to 11.
10. For y from 1 to $h(A) - \Delta$ repeat step 11.
11. if $m(e(a_i), b, (x,y)) < M$ then $M \leftarrow m(e(a_i), b, (x,y))$

   and $c_i \leftarrow \left[\frac{w(A)-\Delta}{2} - x, \frac{h(A)-\Delta}{2} - y \right] R_z \left(-\alpha, \left(x + \frac{\Delta}{2}, y + \frac{\Delta}{2} \right) \right) b$.

12. $\alpha \leftarrow \alpha + \partial\alpha$.

When the above algorithm terminates, C contains the template-based solution for the image alignment.

The upper limit for the complexity of the regular polygonal template matching algorithm is given by

$$n \min(w(A), h(A)) t$$

in the number of matching measurements.

Since the inequality $w(A), h(A) > n$ usually holds for real applications, the template-based method is theoretically slower than the similarity-based one. However, the template representation offers the following possibilities for faster implementations:

• The template images do not need to be actually transformed; the template can be simply redrawn in a different position/orientation, which is computationally cheaper.

• Just the pixels corresponding to the white pixels of templates have to be visited; thus, the coordinates of those white pixels can be stored reducing the area to be scanned.

The simplifications above where explored in the implementation evaluated. That caused the template-based method to be faster than the similarity-based one for the case of regular polygons.

The above algorithm can be easily adapted to deal with more complex templates, like rectangles. The case of matching rectangular templates is tested in this work. However, since rectangles are characterized by two dimensions (width and height) instead of one (radius), the complexity of an algorithm for matching rectangular templates is correspondingly larger.

4 Results

The algorithm was implemented in C++. All tests were executed in a machine with a 133 MHz AMD 586 proces-

sor with a 256 Kbytes cache memory and 16 Mbytes of RAM running Windows 95 with interactive load [Hennessy and Patterson (1990)].

The alignment of regular polygonal objects was evaluated using the images shown in Figure 4. Those images were presented as the input set A to the programs corresponding to both methodologies.

Figure 5 shows the solution for the image alignment problem presented by the similarity-based methodology. A visual inspection indicates that images 1, 2 and 3 are aligned to each other, though the misalignment of images 4 and 5 is noticeable.
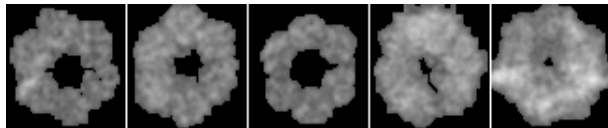

Figure 4: the input set A of images used for the evaluation of the methodologies when processing regular polygonal objects. These images where extracted from the micrograph shown in Figure 2 using the techniques described in [Campos and Coelho (1996)].

Figure 6 shows the template matching. It is important to note that images 4 and 5 have a shape somewhat different from that of a hexagon due to lack of precision in the segmentation process. However, the fitting of the hexagons is very good even for those images. Features not corresponding to hexagons are simply discarded by the matching template.

As pointed out in the previous section, the template-based method described here can be easily adapted to deal with more complex templates. The image input set presented in Figure 7 is used for evaluating the methodologies for rectangles. Figure 8 shows the results using both methodologies with the same input set.

Qualitative evaluations cannot supply strong evidence favoring one method or another. Therefore, the rest of this section discusses quantitative techniques for evaluating the quality of each method.

| 1 | 2 | 3 | 4 | 5 |
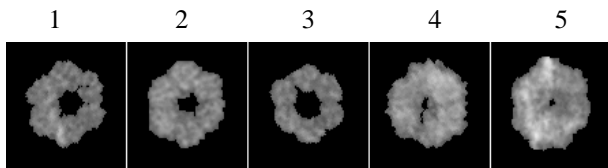
Figure 5: a solution for the image alignment problem of the image set introduced by Figure 4. Image 2 was the one chosen by the algorithm as a reference.
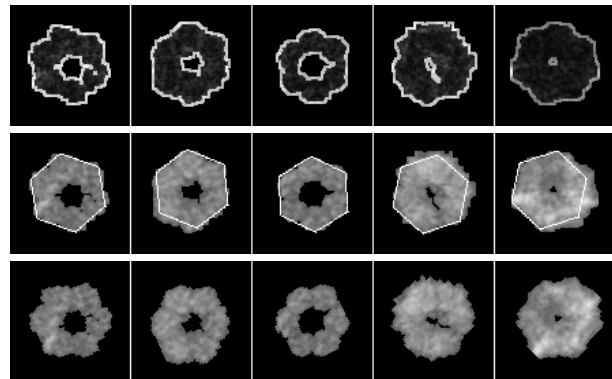
Figure 6: result of the application of the edge detection to the image set (top); best hexagons defined for each image drawn over them (middle); alignment performed by using the transforms given by the hexagons (bottom).
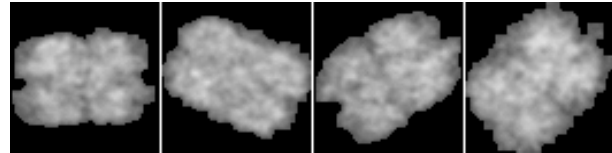
Figure 7: the input set A used for the evaluation of the methodologies in the case of rectangular objects. Images extracted from Figure 2 using the segmentation techniques described in [Campos and Coelho (1996)].
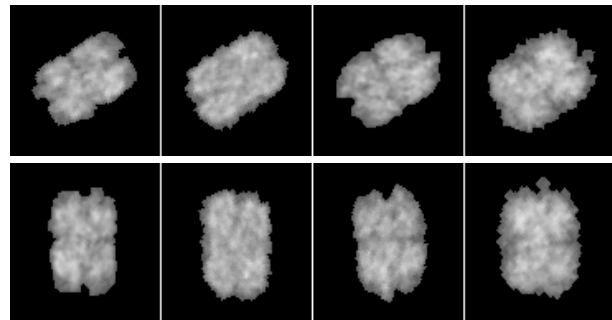

Figure 8: the alignment of the input set presented in Figure 7 by the similarity-based method (top) and by the template-based method (middle).

As mentioned before, the main objective in the alignment of images of quaternary protein structures is the image averaging phase. Hence, the averaged images will be used for quantitative evaluation of the methodologies presented. The average $\overline{a}$ of an image set A has $h(A) \times w(A)$ pixels with intensities given by

$$\overline{a}[x,y] = \frac{\sum_{i=1}^{n} a_i[x,y]}{n} \; .$$

Figure 9 shows the averaging of the images of both input sets aligned by both methodologies.
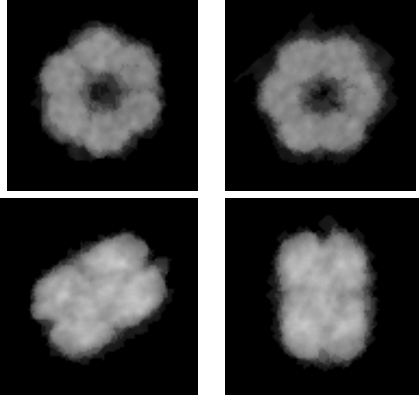
Figure 9: image averaging for the images aligned by the similarity-based method (left) and by the template-based method (right).

Symmetry is the main characteristic of protein quaternary structures. Therefore, an evaluation parameter based on this characteristic was defined. Since the regular polygonal case studied has a sixfold rotational symmetry, it is expected that the rotations of the averaged image around its center by $k\pi/3\,rad, k = \{0,1,2,3,4,5\}$ would be equal to each other. Therefore, the sum of the Euclidean distances between the described rotations is used as a measurement of quality of alignment methodologies results. This measurement can be formally defined as

$$q(\overline{a}) = \sum_{i=0}^{n-2} \sum_{j=i+1}^{n-1} d\left(R_z\left(\frac{i\pi}{n/2},(x,y)\right)\overline{a}, R_z\left(\frac{j\pi}{n/2},(x,y)\right)\overline{a} \right).$$

Clearly, $n=6$ for the case of hexagonal polygonal objects and $n=2$ for the case of rectangular objects.

The point (x,y) used as the center of rotation is different for each case. For the average of the images aligned by similarity, the center of mass of the average was used. For the average of the images aligned by template matching, the geometric center of the image was used, where all the aligned images are positioned by the template-based method.

Sharpness can also be used as a metric. The result of averaging a misaligned set of images is expected to be blurred, while the averaging of well-aligned images tends to be well defined, with sharp features. Since sharpness is related with "bright" edges, a simple way to compute "sharpness" would be the total sum of pixel intensities of the result of applying a border detector over the image. Hence, it can be defined the function

$$c(\overline{a}) = \sum_{x=1}^{w(A)} \sum_{y=1}^{h(A)} e(\overline{a})[x,y].$$

The table below summarizes the results after applying the proposed evaluation metrics. It can be seen that, for hexagonal objects, the template-based method has slightly higher quality than the similarity-based -- 1,6% under the $c(\overline{a})$ measurement, but presents a significant difference (18,8%) with the $q(\overline{a})$ measurement. However, for the case of objects modeled by rectangles, the similarity-based methodology is slightly better using both parameters – a quality 9,3% lower using the symmetry criterion and 5,4% lower using the sharpness criterion. More experimental data is needed in order to reach a final conclusion.

		Metric	
		$q(\overline{a})$	$c(\overline{a})$
Similarity-Based	Hexagon	54850	220727
	Rectangle	1119	165295
Template-Based	Hexagon	46178	224358
	Rectangle	1223	156851

Differences between the performances for hexagonal and rectangular template matchings are also seen in terms of computational efficiency. The table below shows execution time for both methodologies for hexagonal objects. The average time for the template-based method was 459.2 seconds, while the same average for the similarity-based methodology is 517.9 seconds - a difference of about 12.8%.

CPU Time (s)	
Similarity-based	Template-based
948	419
465	453
491	427
446	343
439	353
447	534
514	560
453	625
452	451
551	427
Average: 517.9	Average: 459.2

However, as predicted by the complexity analysis, the template-based method is very time consuming in the case

of rectangular templates. In fact, while the similarity-based method also spent some hundreds of seconds while aligning the rectangular objects, the template-based method spent some hours.

4. Conclusions and Future Work

The methodology based in template matching introduced here showed good results in terms of quality of the final result and mainly in terms of computational efficiency for the case of regular polygonal objects. However, the complexity analysis and results for the case of rectangular templates shows that the template-based method for more complex objects is much more time-consuming than the standard similarity-based method. Preliminary results obtained also rises the suspect that the quality of the template-based alignment for such objects can also be of lower quality.

A future improvements can possibly avoid these great differences of computational efficiency among the different templates used. That improvement would probably come from the use of local instead of global and exhaustive search for template matching. The local search could be done by using gradient search techniques.

However, considering those classes of objects with polygonal projections, the methodology can also be extended through slight modifications to solve problems unrelated to image alignment. Image segmentation, as well as pattern recognition and classification, are suitable to the template matching approach presented here. They represent another promising areas for future work.

References

Ballard, D. H. and C. M. Brown, "Computer vision", 1st, Prentice-Hall, Inc., 1982.

Barrera, J. and G. J. F. Banon, "Bases da Morfologia Matemática Para a Análise de Imagens Binárias", UFPE-DI, 1994.

Castleman, K. R., "Digital Image Processing", Prentice Hall, 1979.

Craig, J. J., "Introduction to robotics: mechanics and control", 2nd, Addison-Wesley Publishing Company, Inc., 1989.

Gilbert, W. J., "Modern Algebra with Applications", John Wiley & Sons, 1976.

Harauz, G. and E. J. Boekema, "Processing and Analysis of Electron Images of Biomolecules", Book, D. D. Haden, C.R.C. Press, 1992.

Hennessy, J. L. and D. A. Patterson, "Computer Architecture: A Quantitative Approach", Morgan Kaufmann, 1990.

Machado, A. M. C., "Metodologias para Reconhecimento de Padrões em Visão Computacional", M. Sc. Thesis, Departamento de Ciência da Computação, Universidade Federal de Minas Gerais, Belo Horizonte, Brazil, 1994.

Pavlids, T., "Algorithms for Graphics and Image Processing", Computer Science Press, 1982.

Radermacher, M., "Three-Dimensional Reconstruction of Single Particles in Electron Microscopy", Book, D. D. Haden, CRC Press, 1992.

Rogers, D. F., "Procedural Elements for Computer Graphics", McGraw-Hill Book Company, 1985.

Rosenfeld, A. and A. Kak, "Digital Picture Processing", Volume 2, 2nd Edition, Academic Press, Inc., 1982.

Stannard, L. (1995). Principles of Virus Architecture. http://www.uct.ac.za/depts/mmi/stannard/virarch.html, University of Cape Town, South Africa.

Steven, A. C. and M. A. Navia, "Fidelity of structure representation in electron micrographs of negatively stained protein molecules", *Proceedings of the National Academy of Sciences of the United States of America* **77**(8), 4721-5.

Van Heel, M. et al., "Electron cryomicroscopy and angular reconstitution used to visualize the skeletal muscle calcium release channel", *Nature - Structural Biology* **2**(1), 18-24.